NBSIR 73-404

Mass Transport and Physical Properties of Large Crystals of Calcium Apatites: Studies of Ca(OH)$_2$ Crystals for use in Electrolytic Conversion of Calcium Fluorapatite Crystals to Calcium Hydroxyapatite

A. D. Franklin and K. F. Young

Inorganic Materials Division
Institute for Materials Research
National Bureau of Standards
Washington. D. C. 20234

September 1, 1972 – August 31, 1973

Annual Report

Prepared for
Department of Health, Education, and Welfare
National Institutes of Health
National Institute of Dental Research
Bethesda, Md. 20014

Interagency Agreement No. Y01–DE–30010

NBSIR 73–404

MASS TRANSPORT AND PHYSICAL PROPERTIES OF LARGE CRYSTALS OF CALCIUM APATITES: STUDIES OF Ca(OH)$_2$ CRYSTALS FOR USE IN ELECTROLYTIC CONVERSION OF CALCIUM FLUORAPATITE CRYSTALS TO CALCIUM HYDROXYAPATITE

A. D. Franklin and K. F. Young

Inorganic Materials Division
Institute for Materials Research
National Bureau of Standards
Washington, D. C. 20234

September 1, 1972 – August 31, 1973

Annual Report

U. S. DEPARTMENT OF COMMERCE, Frederick B. Dent, Secretary

NATIONAL BUREAU OF STANDARDS, Richard W. Roberts, Director

ABSTRACT

In order to convert single crystals of calcium fluorapatite to calcium hydroxyapatite, an electrolytic cell technique will be explored. To utilize such a technique, the cathode compartment must consist of a source of hydroxyl ions and a barrier to the flow of all others. Examination of the literature on metallic hydroxides suggests that a suitable cathode might be composed of an oriented $Me(OH)_2$ crystal, where Me is Mg, Ca, Sr, or Ba, backed up by a Pt electrode in an atmosphere containing H_2O and O_2. $Ca(OH)_2$ crystals have been grown from aqueous solution, and Pt electrodes evaporated onto them. An apparatus has been built to study their ac admittance as a function of temperature and atmosphere, and measurements begun. A computer program for handling the complex admittance data has been devised and tested.

1. INTRODUCTION

Large crystals of calcium hydroxyapatite, $(Ca_{10}(PO_4)_6(OH)_2$, or OHAp) have not yet been grown synthetically, although somewhat impure natural crystals do exist. On the other hand, large crystals of the closely-related calcium fluorapatite $(Ca_{10}(PO_4)_4F_2$, or FAp) and calcium chlorapatite $(Ca_{10}(PO_4)_6Cl_2$, or ClAp) have been grown by the Kyropoulos method (Johnson, 1961), from a flux composed of the corresponding Ca halide (Prener, 1967), and by the Czochralski method (Mazelsky et. al., 1968). All three apatites have closely-related crystal structures (Young, 1967) and the X^- ions in XAp are known to be relatively mobile (Tse et. al., 1972a). This suggests that perhaps large crystals of OHAp can be prepared by replacing F^- in FAp or Cl^- in ClAp crystals by OH^-.

Indeed, Young and Elliot (1966) have succeeded, by annealing ClAp in steam at 1000°C, in replacing all but about 6% of the Cl^- with OH^- ions. However, such a diffusion-controlled process would produce a flux of Cl^- ions out of the crystal, and OH^- ions in, that would eventually decrease exponentially with time, and would therefore take an almost infinite amount of time to replace the last traces of Cl^- ions with OH^- ions.

This difficulty could be obviated by using an electrolytic technique, in which an electric field is applied to drive out the F^- or Cl^- and drive in the OH^- ions. The field would impose the same drift velocity on all ions of the same kind, which in a large field can be much greater than the diffusion random-walk velocity. An approximate calculation, given in the Appendix,

suggests that complete replacement of all F^- ions might be accomplished at about 380°C in a few days under an applied field of 10^3 V/cm.

It is therefore the first objective of this project to test the possibility of the electrochemical transformation of large single crystals of FAp to OHAp.

The method to be tried is shown schematically in Figure 1. An electrolytic cell will be constructed with the FAp crystal as the electrolyte, oriented with the applied electric field along the c-axis. The anode compartment will be composed of a thin crystal of CaF_2 plated with Ca metal or with a pressed mixture of CaF_2 and Ca metal, backed by a Pt electrode. It has been shown (Hinze and Patterson, 1973) that the transport number of the F^- ion in CaF_2 is unity in the presence of metallic Ca down to 400°C, and probably lower. The conductivity of oxygen-doped CaF_2 (Rossing, 1966) is shown in the Appendix to be sufficient to allow the desired current to flow.

The first major problem lies with the cathode compartment. A crystal conducting only by OH^- ion transport is needed, and while on structural grounds there are several promising candidates, none is known definitely at present. The initial task in this work is therefore the selection of the cathode material. A suitable material will be fitted with porous electrodes, probably of Pt, capable of catalyzing the reaction

$$2H_2O + O_2 + 4e \rightleftarrows 4OH^-. \qquad (1.1)$$
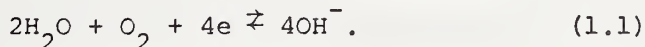
2. CATHODE MATERIALS

  2.1 Literature Study

      A crystalline hydroxide of good stability in the temperature
region from 300-500°C is required, in which there is reason to believe
that OH^- ions exist and are mobile. Among several promising classes
are those with formula MeOOH, where Me stands for Fe or Al, and the
alkaline earth hydroxides with formula $Me(OH)_2$.

    2.1.1 MeOOH

          White (1971) reported studying the transport of OH^-
ions in SiO_2, using geothite (FeOOH) as the cathode material for a
determination of the electrical conductivity. However, in a private
communication he stated that there was no independent information on
the transport number and mobility of OH^- in FeOOH.

      The hydroxy oxides of Al and Fe occur with two distinct structures,
that of boehmite (γ-AlOOH) or lepidocrocite (γ-FeOOH), and that of
diaspore (α-AlOOH) and goethite (α-FeOOH). In all four compounds, the
shortest distances between oxygen ions not part of the same metal-oxygen
octahedron are about 27 nm, and are assumed (Milligan and McAtee, 1956)
to represent hydrogen bonds. This is consistent with data on the infra-
red optical absorption of boehmite (Schwartzmann, 1962; Wickersheim and
Korpi, 1965), which exhibit what are probably O-H stretching bands in
the wavelength region from 3000 to 3300 cm^{-1}. Hydrogen bonds between
two oxygen ions separated by 27 to 27.5 nm generally have their O-H

stretching frequencies in this region (Pimentel and McClellan, 1960).

The existence of distinct hydrogen bonds between the OH^- and O^{2-} ions suggests that charge transfer might take place by proton motion rather than by hydroxyl ion motion. If so, this class of materials would be unsuitable as the cathode compartment material. Fripiat and coworkers have indeed interpreted measurements with boehmite on the temperature dependence of the infrared intensities (1967a), dielectric absorption, electrical conductivity, and proton diffusion (1967b), and proton nmr (1969) on this basis. We have, therefore, chosen not to examine these MeOOH compounds further.

2.1.2 Me(OH)$_2$

The situation is quite different with respect to the alkaline earth hydroxides with the Brucite structure. These crystals belong in the hexagonal system, with the oxygen ions arranged linearly along the $\underline{c}$ axis. The smallest O-O distance is about 3.3 Å in Ca(OH)$_2$ which led Bernal and Megaw (1935) to suggest that no hydrogen bonding takes place. In Mg(OH)$_2$, and also presumably in Ca(OH)$_2$, the O-H bonds also lie along the $\underline{c}$ axis (Elleman and Williams, 1956), with an O-H bond length of about 0.98 Å (Elleman and Williams, 1956; Busing and Levy, 1957; Henderson and Gutkowsky, 1962), quite comparable to that in non-hydrogen-bonded molecules. The vibration corresponding to the O-H stretching frequency, while somewhat complex due to mixing with the lattice modes, occurs (e.g., Buchanan, Caspers, and Murphy, 1963) around 3700 cm^{-1}, where

it would be expected for non-hydrogen-bonded OH^-.

It thus appears that $Ca(OH)_2$ should be a reasonable candidate for an OH^- conductor, and experiments to grow crystals and determine the transport number of the OH^- ion were begun.

Experimental Study of $Ca(OH)_2$

2.2 Crystal Growth

In order to determine the properties of $Ca(OH)_2$, and indeed to utilize this highly anisotropic substance in the cathode compartment of the electrolytic cell for conversion of FAp to OHAp, single crystal plates are necessary of about 1 mm thickness, along the c axis, and several mm^2 area perpendicular to the c axis.

Satisfactory crystals have been grown by the diffusion technique (Ashton and Wilson, 1927) using an apparatus as shown in Figure 2. Ca_2-free water is used, prepared by boiling distilled water slightly acidified with HCl for about 16 hours in a reflux condenser. Air first passed through an ascarite column is slowly bubbled through the water during boiling. The U-tube in Figure 2 is filled with this water, under a protective layer of liquid paraffin, and then NaOH solution, about 27 molar, is carefully pipetted into the bottom of one of the vertical inner tubes and saturated $CaCl_2$ into the bottom of the other, without allowing stirring of the water above these solutions. The NaOH and $CaCl_2$ solutions form distinct, quiescent layers below the water, with initially well-defined interfaces separating them from the water. The NaOH

solution, under paraffin oil, was allowed to stand for at least two days to let any Na_2CO_3 settle out. The $CaCl_2$ solution was prepared with CO_2-free water, slightly acidified, and boiled with CO_2 free air passing through it for 16 hours. It was also stored under paraffin oil.

The crystals grow by interdiffusion of Ca^{2+} and OH^- ions. The OH^- ions travel much more rapidly in aqueous solution than do the other ions, as shown by the values given below for the equivalent conductance of these ions (Chemical Rubber Handbook, 39th Edition):

OH^-	172.0 siemens[*]
Cl^-	65.5
$1/2\ Ca^{2+}$	51.0
Na^+	43.5.

Without special precautions to inhibit the transport of OH^- ions, it was found that the crystals grown (all growth so far has been at room temperature) were acicular in shape, perhaps due to high concentrations of Ca^{2+} ions during growth.

A satisfactory arrangement has been to restrict the transport of OH^- ions by making the orifices (there are four) of the inner tube containing the NaOH solution small, about 1 mm in diameter, while those of the $CaCl_2$ are considerably larger. Under these conditions, small plates of

---

* Siemens is the SI unit for conductance, and equals the previously-used mho, or reciprocal ohm.

$Ca(OH)_2$, several mm across, grow inside the $CaCl_2$ inner tube over a
period of several weeks. As Ca^{2+} diffusion reaches the NaOH chamber,
crystallization occurs at the orifice, eventually blocking it. This
effect limits the size of the crystal obtained at present, but they
should be large enough to allow determination of the OH^- transport in
$Ca(OH)_2$ and to test the feasibility of electrolytic conversion of FAp
to OHAp. The crystals are stored under benzene to protect them from
atmospheric CO_2.

2.3 Electrode Application

The electrodes to be applied to the $Ca(OH)_2$ crystals must serve
a dual purpose. They must not only supply electrons but must also
catalyze the reaction between water, oxygen, and electrons (Eq. 1.1)
to produce hydroxyl ions. Platinum is known to operate in just this
fashion in both aqueous systems and as electrodes in fuel cells reacting
H_2 with O_2 (e.g., Hoare, 1968). Some such cells use an alkaline medium,
such as an aqueous KOH solution and their operation most probably is
very similar to what should occur on our $Ca(OH)_2$ crystals provided the
OH^- ions are mobile. Because of this favorable history and because Pt
can be evaporated reasonably readily, it was decided to begin at least
with evaporated Pt electrodes.

Evaporation of Pt electrodes was done in a vacuum, under a pressure
of a few N/m^2 (a few mm of Hg x 10^{-6}), produced by a diffusion pump
operating through a liquid-nitrogen trap. The crystal was placed in a
copper cup, under benzene, and covered with a nickel plate with a hole

approximately 1-1/2 mm in diameter under which the crystal was positioned.
As the vacuum was established the benzene evaporated, leaving the crystal
ready for deposition of Pt through the hole to form a round electroded
area. During evaporation the cup containing the crystal became quite
warm but no serious decomposition of the crystal was immediately apparent.
The course of the evaporation was monitored by following, with an ohmmeter,
the conductance of the film deposited upon a glass surface placed near the
crystal. While this measurement has not yet enabled us to estimate
quantitatively the film thickness, it has been useful as an indicator
of the onset and continuation of deposition. After evaporation, CO_2-free
air was admitted to the bell jar, the jar lifted away and benzene
quickly added to the cup, immersing the specimen. The crystal was turned
over and the process repeated, to produce Pt electrodes on each of the
basal faces.

Although no damage to the crystals during deposition was immediately
observable, some of the evaporated electrodes have not been firmly attached
to the crystal, and have become detached after a period of time, more or
less as single units. Contributing factors may be deposition of extraneous
material from the benzene bath (ACS certified benzene, thiophene-free,
was used and should leave negligible residue); surface decomposition of
the crystal, with loss of water, either by infrared heating by the hot
filament or by bombardment by hot Pt ions; or surface contamination of
the crystal by CO_2 during handling.

2.4 Electrical Measurements

In order to determine that OH^- ions are the predominant charge carriers in $Ca(OH)_2$ it will ultimately be necessary to compare the total charge, coulometrically determined, with the total quantity of OH^- ions transported in a symmetric dc electrolytic cell. The passage of OH^- ions can be monitored by the disappearance of H_2O and O_2 from one side of the cell and their appearance at the other. However, preliminary measurements are needed to obtain an estimate of the total conductance of the $Ca(OH)_2$, to determine whether it is large enough to maintain the current required for conversion of FAp to OHAp in a reasonable time.

The most useful form of preliminary measurement appears to be an ac measurement of the capacitance and conductance of the $Ca(OH)_2$ crystal, between Pt electrodes deposited upon each side. At sufficiently high frequency, the observed values of capacitance and conductance should be the true values for the crystal, while any blocking of charge carriers at the electrodes should produce a decrease in conductance and a rise in capacitance as the frequency decreases (see e.g., Friauf, 1954). Such measurements, made as functions of H_2O and O_2 content of the atmosphere, could also give information about the proposed catalytic reaction on the Pt electrodes. The temperature should also be varied in the search for a range of variables giving satisfactory performance.

2.4.1 Measurement Cell

The first cell built, which used a ceramic specimen holde proved to be unsatisfactory because of extraneous conduction through

the ceramic holder. The holder shown in Figure 3 was then built, and appears to be giving satisfactory results.

The inner assembly, shown in Figure 3, is enclosed in an external stainless-steel can which bolts to the cover plate with an o-ring seal, so that the atmosphere surrounding the specimen can be controlled. The electrical leads are fed through the cover plate via insulating seals, and since these are kept at room temperature, there is negligible conductance between these leads. The specimen sits upon a silvered Ni plate which makes contact with the lower evaporated Pt electrode of the specimen (in future work a path may have to be provided to allow better atmospheric access to this electrode). The upper Pt electrode is contacted by a spring-loaded nichrome wire fastened electrically to the slack Pt lead wire connecting to the external bridge. The lower portion of the assembly can be inserted into a controlled furnace and the temperature monitored by the Pt/Pt-10% Rh thermocouple near the specimen.

The electrical measurements are made using a Wayne-Kerr B221*bridge, using either the internal oscillator and detector at 1592 Hz or, for varying frequencies, a Krone-Hite 440 AR oscillator and General Radio 1232-A tuned amplifier as a detector. The frequency range available with this arrangement is from about 50 Hz to perhaps 70 kHz, although the latter figure may be pushing the bridge too far.

*Certain commercial equipment, instruments, or materials are identified in this paper in order to adequately specify the experimental procedure. In no case does such identification imply recommendation or endorsement by the National Bureau of Standards, nor does it imply that the material or equipment identified is necessarily the best available for the purpose.

In using the cell, it is necessary to know the capacitance and con-
ductance shunting the specimen. Since the shunt capacitance is expected
to vary with the length of the central lead, measurements were made,
without a specimen, as a function of the distance between the lower plate
contact and the bottom of the upper wire contact. Figure 4 shows that
the shunt conductance is independent of the distance between contacts
but does depend upon frequency. The shunt capacitance, shown in Figure 5,
exhibits a roughly linear dependence for large separation of the contacts
plus a component that rises rapidly as the separation decreases. This
latter component represents the direct capacitance between the contacts
and will be replaced by the specimen capacitance during the actual measure-
ment. Hence, correction of the experimental data for the shunt capacitance
introduced by the cell requires the linear component only, extrapolated
to a contact separation equal to the specimen thickness.

The frequency dependences of the linear component of the shunt capacitance
at three values of the contact separation and of the shunt conductance
are shown in Figure 6. There is no dependence upon temperature. When
the bridge is used to measure the equivalent parallel capacitance and
conductance of the crystal, appropriate numbers from this Figure 6 can be
subtracted from the measured data to yield values for the specimen
alone. For the shunt capacitance, interpolation to the correct specimen
thickness is needed.

2.4.2 Measurements on Crystals

Measurements have been made on two crystals. Due to the
small amount of data obtained as yet, and the evidence for atmospheric

attack upon the specimens, to be discussed, these measurements are only of a very preliminary nature.

Figure 7 shows equivalent parallel capacitance and conductance data obtained at 345°C on a $Ca(OH)_2$ crystal in the earlier specimen holder. Because in this specimen holder the shunt admittances were large, the values attributable to the specimen are rather uncertain, particularly the conductance above about 10 Hz. However, a relaxation appears centered around 600 Hz. These data appeared to be independent of the atmosphere, whether dry "CO_2-free" air or nitrogen, or air or nitrogen bubbled through "CO_2-free" water held at room or ice temperatures. A very similar curve was found for a second crystal in the improved specimen holder described here, held at 335°C in dry "CO_2-free" air, as shown in Figure 8. For both crystals at room temperature, essentially no equivalent parallel capacitance or conductance was found. The electrode areas are very small, of the order of 10^{-2} cm^2, and the specimen thickness about 5×10^{-2} cm, so that the true capacitance could not have been greater than about 0.1 pF. The much larger values seen in Figures 7 and 8 undoubtedly arise from the blocking of charge carriers at the electrodes.

During these measurements, and particularly those for the second crystal, Figure 8, it became apparent that irreversible changes were taking place in the crystals, and upon subsequent examination they were found to have undergone extensive attack by CO_2. The electrical data

may well have been influenced by this attack, and more stringent precautions in eliminating CO_2 from the atmosphere will be required.

2.5 Atmosphere Control

Most of the measurements were made in wet or dry air that had been passed through a column packed with an NaOH-asbestos mixture, about 15 cm long. This "CO_2-free" air when bubbled, via a fine glass frit, through a saturated solution of $Ba(OH)_2$ for several days produced no visible precipitate, whereas without the ascarite column a precipitate was formed. On the other hand, when the "CO_2-free" air was passed over $Ba(OH)_2$ crystals held at room temperature, attack was soon noted and in a few days the $Ba(OH)_2$ appeared to be completely converted to $BaCO_3$.

This apparent great reactivity of the alkaline earth hydroxides in crystal form is demonstrated by another observation. $Ca(OH)_2$ crystals kept under ethyl alcohol exhibited signs of CO_2 attack after days or weeks. Needles were much more rapidly attacked than plates, and in both cases the faces parallel to the c axis seem to be particularly reactive. In future experiments, tank gases will be used instead of air, and rigid precautions will be taken to remove and monitor CO_2.

3. COMPUTER PROGRAM FOR HANDLING DIELECTRIC DATA

The equivalent parallel admittance of a slab specimen with blocking electrodes is expected in general to be a complex function of frequency, but under most conditions of experimental interest to be well represented (c.f., Raleigh, 1968) by a simple Debye-type expression

$$Y_p = \frac{iwC_o}{1+iwR_oC_o} \qquad (1)$$

where w is 2π times the frequency, and C_o and R_o are the low-frequency limit of the capacity and the high-frequency limit of the resistance. A simple interpretation is that the crystal behaves like an equivalent circuit with a resistor R_o in series with a capacitor C_o, or like a block of conductive material of resistance R_o between two identical capacitors of value $2C_o$, representing the blocking electrodes. Charge is stored in each cycle at the electrode-electrolyte interface, and energy lost by the passage of the current through the resistive material.

When this equivalent parallel admittance is plotted in the complex plane, a semi-circular arc is obtained with its center on the real axis, analogous to the Cole-Cole plot (Cole and Cole, 1942) used in treating dielectric constant data. Bauerle (1969) has shown for experiments with calcia-stabilized zirconia solid-state electrolytes with porous Pt electrodes in oxygen atmospheres that several over-lapping arcs appear, with centers somewhat below the real axis. The several arcs can be individually attributed to electrode and bulk processes.

At constant temperature Bauerle found that the electrode resistance decreased with increasing oxygen pressure, behavior that parallels our expectations for the behavior of our system of $Ca(OH)_2$ with Pt electrodes in an H_2O/O_2 atmosphere. The depression of the arcs below the real axis suggests a small distribution of electrode and bulk process parameters, which plays a role similar to that of the distribution of relaxation times in the treatment of the dielectric constant (Cole and Cole, 1942).

Experience in this laboratory with disentangling the several overlapping arcs that can appear in treatments of data such as this has suggested the utility of having a general, numerical method of fitting the overall data to a sum of the contributions from several separate mechanisms, each of which alone would produce a single arc. We describe next a computer-based technique for performing such fits. In electrode polarization problems, the data would be most apt to produce a pattern of arcs when plotted in the complex plane of the admittance,

$$Y(w) = G(w) + iB(w), \qquad (2)$$

although dielectric relaxation problems would most likely be dealt with in terms of the complex capacitance

$$C(w) = \varepsilon_o \varepsilon' C_o - \varepsilon_o i \varepsilon'' C_o. \qquad (3)$$

In these equations, G and B are the conductance and susceptance, ε_o the dielectric constant of free space, ε' and ε'' the real and imaginary

parts of the relative complex dielectric constant, and $\varepsilon_o C_o$ the air

capacitance. We discuss our data-handling technique in terms of the

complex capacitance, $C^* = C' - iC''$, $C' = \varepsilon_o \varepsilon' C_o$ and $C'' = \varepsilon_o \varepsilon'' C_o$,

but it can readily be adapted to use with the complex admittance Y,

or any other similar quantity.

An electronic calculator with a plotter attachment and magnetic

tape cassette memory is used in the processing and display of

the data.

These data are collected as functions of frequency, temperature,

and composition of the controlled gaseous environment of the specimen.

The ease, accuracy, and flexibility of graphically displaying these

data in the complex plane not only allows the structure of the data to

be revealed, but also their dependence on temperature and the nature of

the gaseous environments by plotting families of curves on the same

graph. Selected regions of the graphs can be expanded if necessary, and

graphs of a summary nature or for publication purposes can be quickly

prepared. The data are stored on magnetic tape in cassettes and can be

quickly recalled and re-plotted for comparison purposes.

When the specimen exhibits a single charge-storage mechanism obeying Eq. (1),

only one arc is produced in the complex plane, and the data can be fitted

to such an arc by minimizing the sum of the squares of the radial deviations

of the data from the arc. From this arc we then obtain the limiting high and

low frequency values of capacitance (C_o, C_∞), a most probable relaxation time

(τ) and two parameters (m and n) representing the distribution of relaxation times for that mechanism. The process of fitting also reveals the presence of more than one mechanism should they exist. Each arc, arising from a single mechanism but with, in general, a distribution of relaxation times, may be represented by

$$C^* - C_\infty = \frac{\Delta C}{1+i^n (w\tau)^m} \tag{4}$$

where: C^* = complex capacitance = $C'-iC''$; $\Delta C = C_o - C_\infty$; w = angular frequency. Then

$$\left\{ \frac{(C_o-C')^2 + C''^2}{(C'-C_\infty)^2 + C''^2} \right\}^{1/2} = (w\tau)^m \equiv W \tag{5}$$

and the depression, D, of the center of the arc below the real axis is

$$D = \frac{\Delta C}{2} \operatorname{Cot} \frac{n\pi}{2} \tag{6}$$

and the slope of ℓnW <u>vs</u> ℓnw is equal to m:

$$\ell nW = m\ell n\tau + m\ell nw \tag{7}$$

For a relaxation mechanism with a single relaxation time, D is zero and m is equal to unity.

If it appears that there are two or more mechanisms (two or more superimposed arcs) present, then the dominant one may be fitted by the least-squares technique described above, and using equation (4) above, the contribution from that mechanism may be subtracted from the raw data. The difference constitutes a new set of data which is presumably due to all other mechanisms and should itself be suitable for the least-squares fitting procedure just used provided one of the remaining mechanisms again dominates the rest. If so, the process may be repeated, removing this second contribution from the raw data, and so on. When all the data have been fitted, the entire scheme may be repeated any number of times, to refine the fit. The whole is an iterative process that converges on the best possible fitted values by eliminating as far as possible the interference of one mechanism with another. This procedure works quite well when dealing with such systems as treated in Bauerle's study of solid electrolyte polarization (Bauerle, 1969).

4. FUTURE PLANS

Several experimental problems need to be solved in order to complete the study of $Ca(OH)_2$ as a potential cathode material. These include the deposition of reproducible Pt electrodes without crystal damage and the provision of an atmosphere without damaging CO_2 for electrical measurements at elevated temperatures.

Once solutions to these problems are in hand, the task of determining the electrical properties of $Ca(OH)_2$ crystals and finding the conditions under which electrodes reversible to the generation and absorption of OH^- ions can operate can proceed. Preliminary experiments have shown that sizeable $Ba(OH)_2$ crystals can be formed, so the techniques already set up can probably be used with little modification to screen $Sr(OH)_2$ and $Ba(OH)_2$ crystals as well, if need be.

If reversible electrode action can be achieved in one of these crystals that exhibits a satisfactory level of conductivity it will then be necessary to proceed to determining the OH^- transport numbers, and beyond that the experiment to replace F^- ions in FAp with OH^- ions to produce OHAp.

5. APPENDIX

   5.1 Estimation of the Time to Replace F^- Ions in FAp With OH^- Ions.

   In the hexagonal crystal structure of FAp, the F^- ions lie in chains parallel to the c-axis. The chains intersecting a given basal plane form a hexagonal pattern.

   Let N_c = Number of chains per cm^2 of basal plane

   L = Thickness of crystal, or length of chain

   N_v = Number of vacant F^- sites per cm^3

   n_v = Number of vacant F^- sites per cm of chain

   r_L = distance between F^- sites along the chain

   r_a = distance between chain intersections on the basal plane.

Then

$$N_c = 2/[\sqrt{3}\ r_a^{\ 2}]$$

$$n_v = N_v/N_c$$

The flux of vacancies, and therefore F^- ions, passing through a given basal plane along a single chain is

$$F = n_v \mu E$$

where μ is the vacancy mobility and E the applied field. The number of

ions in the length L is L/r_L, so that the time to exchange the entire length is

$$\tau = \frac{L}{Fr_L} = \frac{LN_c}{r_L N_v \mu E} = \frac{2L}{\sqrt{3} r_L r_a^2 N_v \mu E}$$

The conductivity is given by

$$\sigma = N_v \mu e$$

where e is the elementary charge.

The familiar ionic-crystal equation for the mobility μ may be written (Lidiard, 1957)

$$\mu = \frac{r_L^2 e}{kT} \ \nu \exp(\Delta s_m/k) \ \exp(-\Delta h_m/kT)$$

where k is Boltzmann's Constant, T the Kelvin temperature, ν the vibrational frequency of an ion next to a vacancy, and Δs_m and Δh_m the entropy and enthalpy of activation for the jump of the neighboring ion into the vacancy.

Numerical values to put into these formulae can at least be estimated. Arends et. al. (1968) estimate the number of vacancies per cm^3 in OHAp to be about 10^{19}, and we adopt that for N_v for FAp also. Prener (1967)

gives r_L = 3.45x10^{-8} cm and r_a = 9.36x10^{-8} cm. A thickness (L) of 1 cm

for the crystal and an applied electric field of 10^3 V/cm will be assumed.

The vibrational frequency ν of the F$^-$ ions must be below about 8x10^{12} sec^{-1}

($\sim$ 240 cm^{-1}) since Baddiel and Berry (1966) explored the infrared vibrational

spectrum as far down in frequency as 250 cm^{-1} apparently without finding

the lattice vibrations. Typical values for this frequency (c.f., Donovan

and Angress, 1971) in relatively ionic crystals run from about 2x10^{12}

to 10^{13} sec^{-1}. For the purposes of this estimation, a value of

5x10^{12} sec^{-1} will be used. Tse, Welch, and Royce (1972a) report a

value of 0.78 eV for Δh_m, the enthalpy of motion of the F$^-$ vacancy in

FAp, although they estimate (1972b) on theoretical grounds that Δh_m

for the OH$^-$ ion must be larger. We will use 0.78 eV, but must recognize

that for the OH$^-$ ion motion may be slower and the ionic replacement

process therefore take longer than we estimate here. The entropy of

motion, Δs_m, is more difficult to estimate. However (c.f., Franklin,

1972) in most ionic crystals $\Delta s/k \sim 1$ to 3 for vacancy motion. We will

choose $\Delta s \sim k$ here.

With these values we find that at 380°C the mobility μ is about

2.8x10^{-7} cm^2/volt·sec at 380°C, and the conductivity is about

1.5x10^{-6} ohm^{-1}cm^{-1}. The time to completely exchange a crystal 1 cm

thick at this temperature would then be about 16 days.

This is a very crude estimate. The calculated replacement time is a

long but not impossible time. It may be a low estimate because of the

possibility that the mobility of OH^- ions is less than that of F^- ions. On the other hand, somewhat higher temperatures should be possible, and crystals only a tenth of a cm thick would still be suitable for most physical property measurements.

REFERENCES

Ashton, F. W. and Wilson, R., 1927, Am. J. Science 13, 209.

Baddiel, C. B. and Berry, E. E., 1966, Spectrochim. Acta 22, 1407.

Bauerle, J. E., 1969, J. Phys. Chem. Sol. 20, 2657.

Bernal, J. D. and Megaw, H. D., 1935, Proc. Roy. Soc. A151, 384.

Buchanan, R. A., Caspers, H. H., and Murphy, J., 1963, J. Appl. Optics
    2, 1147.

Busing, W. R. and Levy, H. A., 1957, J. Chem. Phys. 26, 563.

Cole, K. S. and Cole, R. H., 1942, J. Chem. Phys. 10, 98.

Donovan, B. and Angress, J. F., 1971, Lattice Vibrations, (Chapman
    Hall, Ltd., London) p. 98.

Elleman, D. D. and Williams, D., 1956, J. Chem. Phys. 25, 742.

Franklin, A. D., 1972, in Point Defects in Solids, J. H. Crawford, Jr.
    and L. M. Slifkin, Ed. (Plenum Press, N.Y.) p. 76.

Fripiat, J. J., Bosmans, H., and Rouxhet, P. G., 1967, J. Phys. Chem.
    71, 1097.

Fripiat, J. J. and Touillaux, R., 1969, Trans. Far. Soc. 65, 1236.

Henderson, D. M. and Gutowsky, H. S., 1962, Am. Mineral. 47, 1231.

Hoare, J. P., 1968, The Electrochemistry of Oxygen, (Interscience, New
    York) p. 307.

Lidiard, A. B., 1957, Handbuch der Physik, Vol. 20, S. Flügge, Ed.,
    (Springer-Verlag, Berlin) p. 246.

Mata Arjona, A. and Fripiat, J. J., 1967, Trans. Far. Soc. 63, 2936.

Milligan, W. O. and McAtee, J. L., 1956, J. Phys. Chem. 60, 273.

Pimentel, G. C. and McClellan, A. L., 1960, The Hydrogen Bond

(Freeman, San Francisco) Fig. 3-9.

Prener, J. S., 1967, J. Electrochem. Soc. 114, 77.

Raleigh, D. O., 1968, J. Phys. Chem. Soc. 29, 261.

Schwartzmann, E., 1962, Z. Anorg. Chem. 317, 176.

Tse, C., Welch, D. O., and Royce, B. S. H., 1972a, Bull. Am. Phys. Soc.,

Ser. II, 17, 265, Paper BH5; 1972b, Bull. Am. Phys. Soc., Ser. II,

17, 265, Paper BH4.

White, S., 1971, Nature 230, 192.

Wickersheim, K. A. and Korpi, G. K., 1965, J. Chem. Phys. 42, 579.

FIGURE CAPTIONS

1. Schematic diagram of cell for electrolytic conversion of FAp to OHAp.

2. Schematic diagram for growth of $Ca(OH)_2$ crystals by diffusion.

3. Cell for ac electrical measurements of $Ca(OH)_2$ crystals.

4. Dependence of the shunt conductance of the electrical cell of Figure 3 upon interelectrode spacing at three measurement frequencies. The units of conductance are picosiemens (see footnote, p. 7).

5. Dependence of the shunt capacitance of the electrical cell of Figure 3 upon interelectrode spacing at three measurement frequencies.

6. Dependence of the shunt capacitance and conductance of the electrical cell of Figure 3 upon measurement frequency. The units of conductance are picosiemens (see footnote, p. 7).

7. Frequency dependence of capacitance and conductance of $Ca(OH)_2$ crystal 111-1 at 345°C in all atmospheres. The units of conductance are nanosiemens (see footnote, p. 7).

8. Frequency dependence of capacitance and conductance of $Ca(OH)_2$ crystal 111-2 at 335°C in dry air. The units of conductance are nanosiemens (see footnote, p. 7).

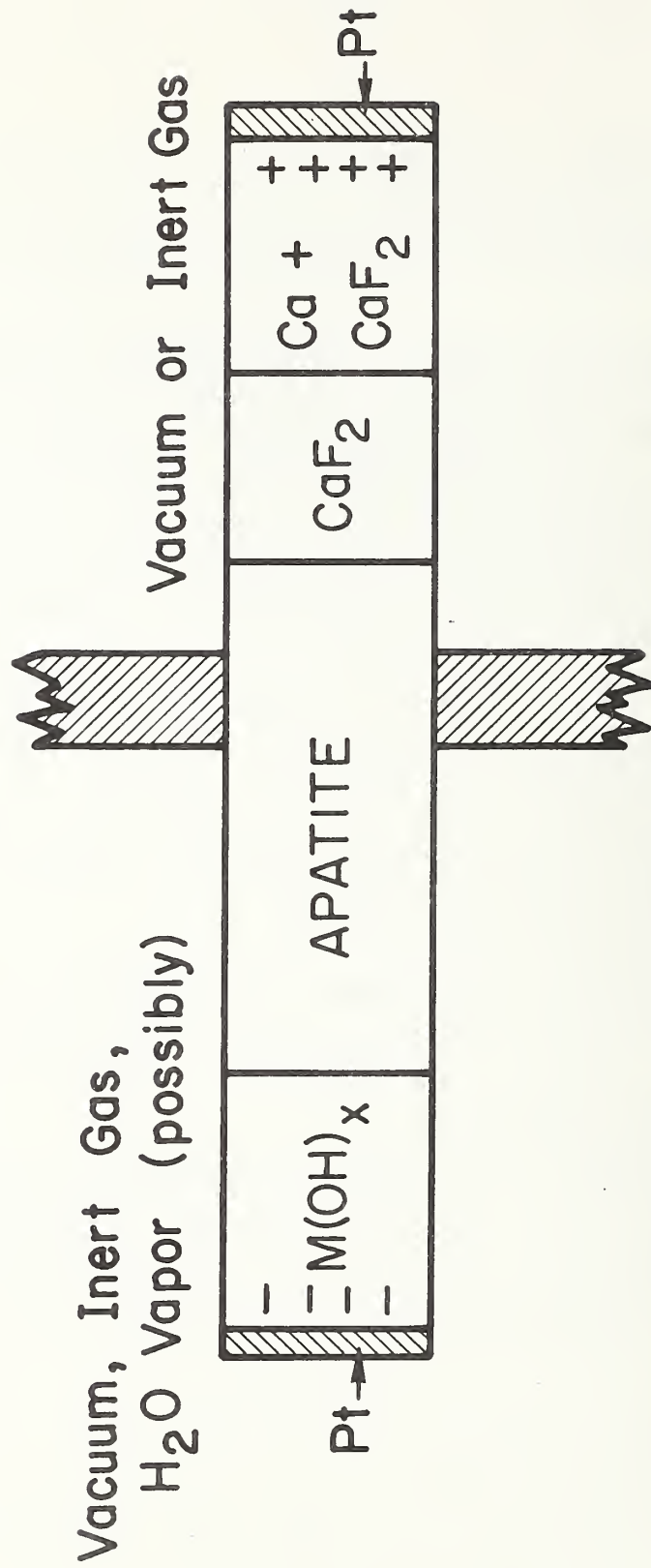Fig. 1. Schematic diagram of cell for electrolytic conversion of FAp to OHAp.
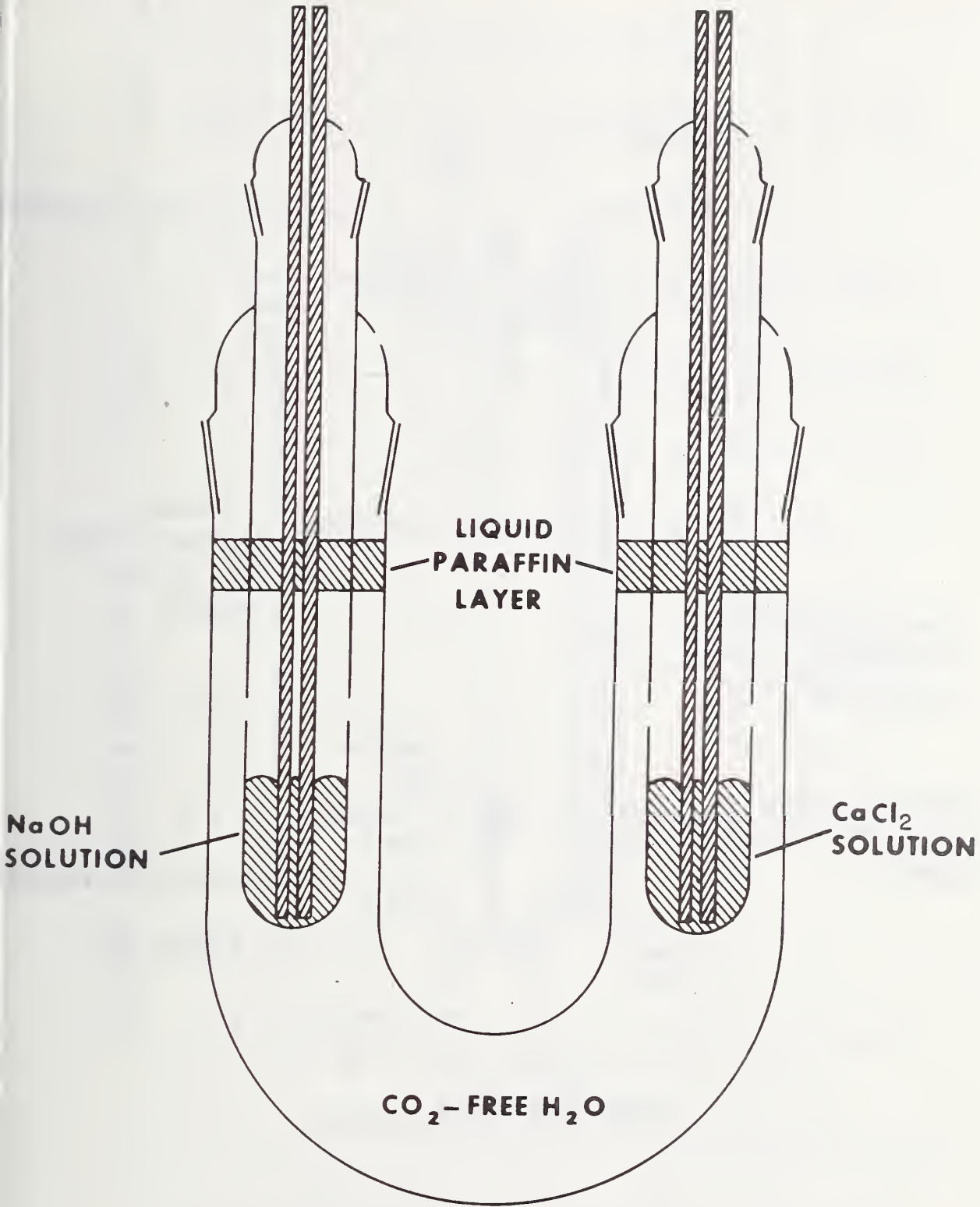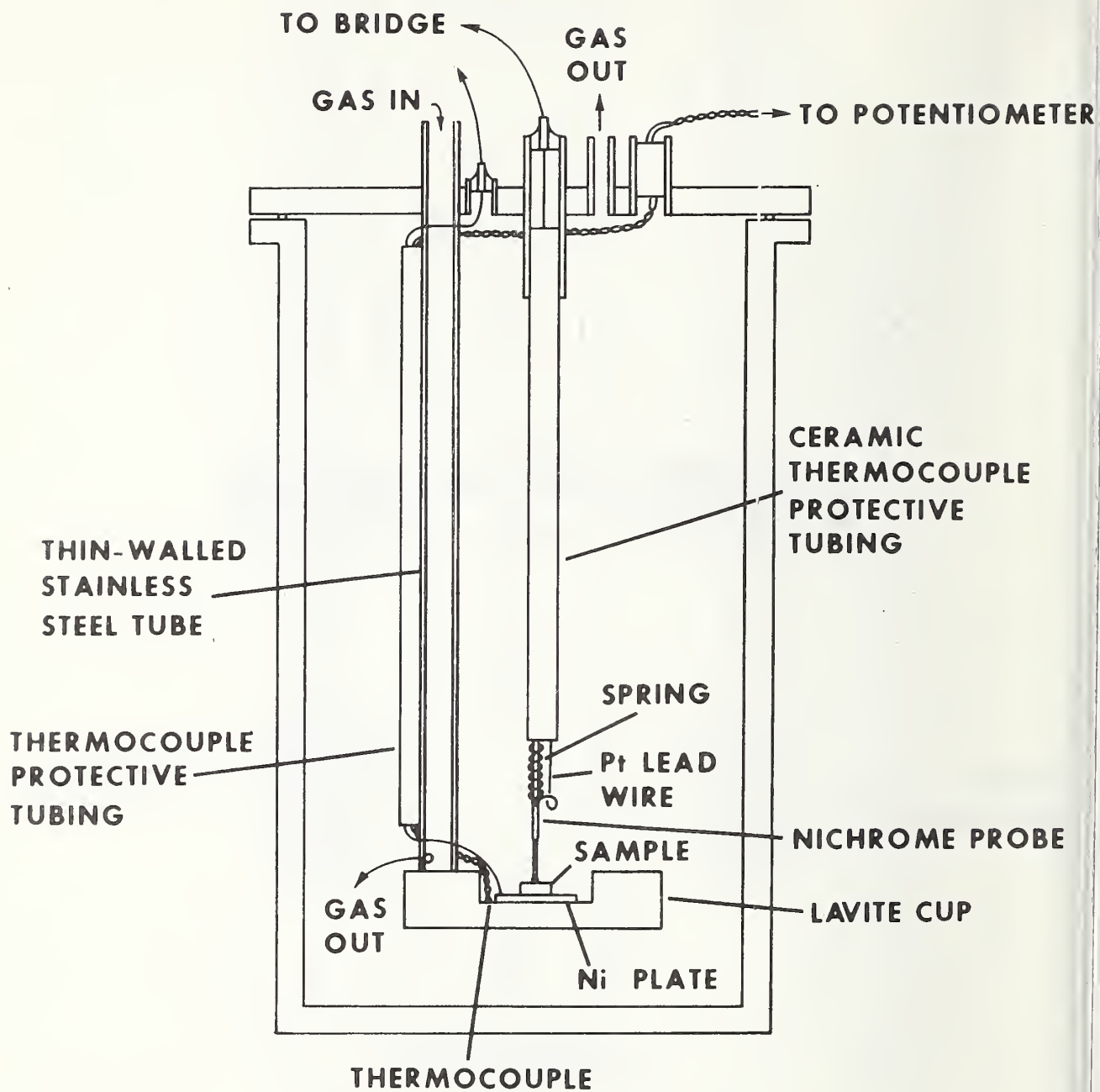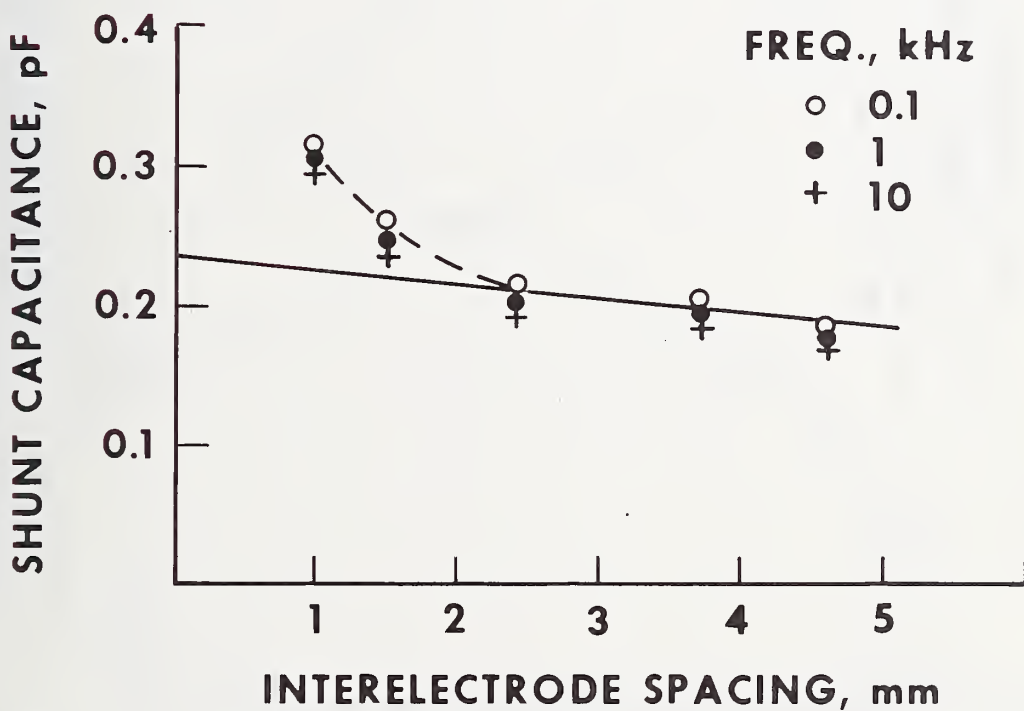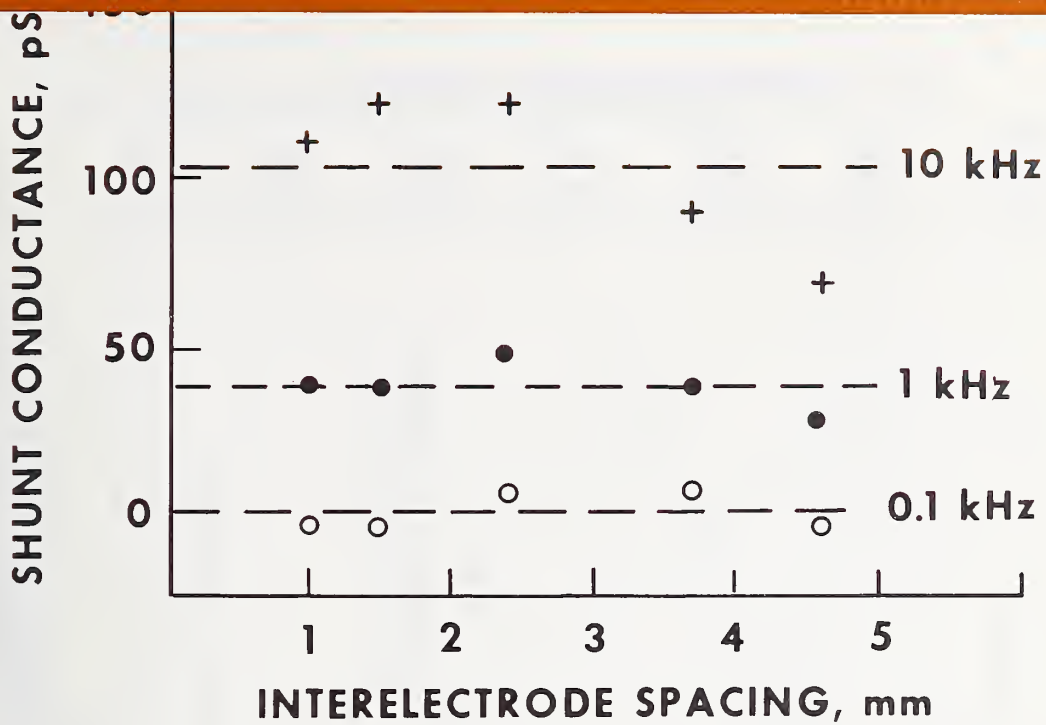
LIQUID
PARAFFIN
LAYER

NaOH
SOLUTION

CaCl$_2$
SOLUTION

CO$_2$-FREE H$_2$O

Fig. 2. Schematic diagram for growth of Ca(OH)$_2$ crystals by diffusion.

Fig. 3. Cell for ac electrical measurements of Ca(OH)$_2$ crystals.

Fig. 4. Dependence of the shunt conductance of the electrical cell of Figure 3 upon interelectrode spacing at three measurement frequencies. The units of conductance are picosiemens (see footnote, p. 7).

Fig. 5. Dependence of the shunt capacitance of the electrical cell of Figure 3 upon interelectrode spacing at three measurement frequencies.
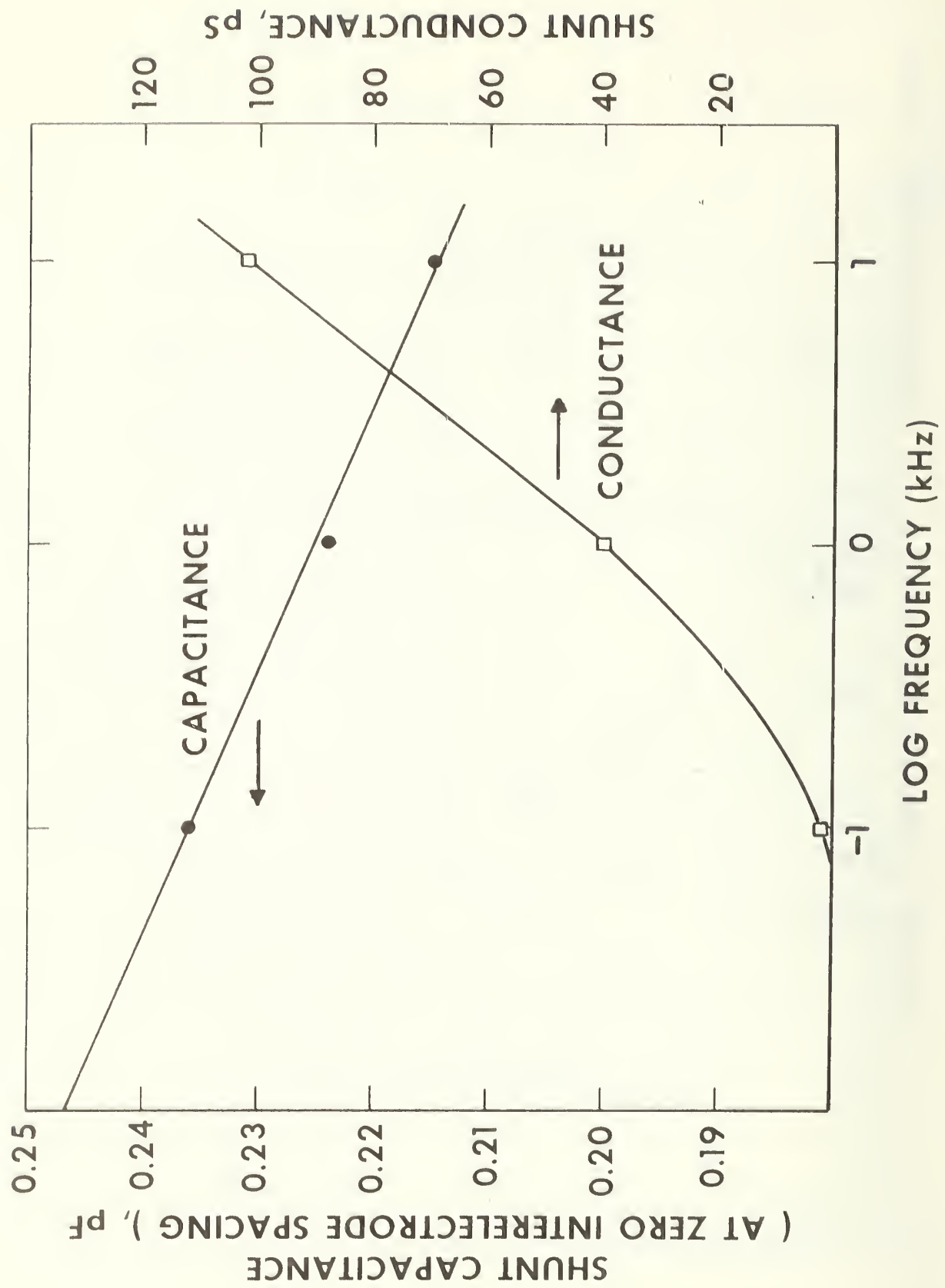
Fig. 6. Dependence of the shunt capacitance and conductance of the electrical cell of Figure 3 upon measurement frequency. The units of conductance are picosiemens (see footnote, p. 7).
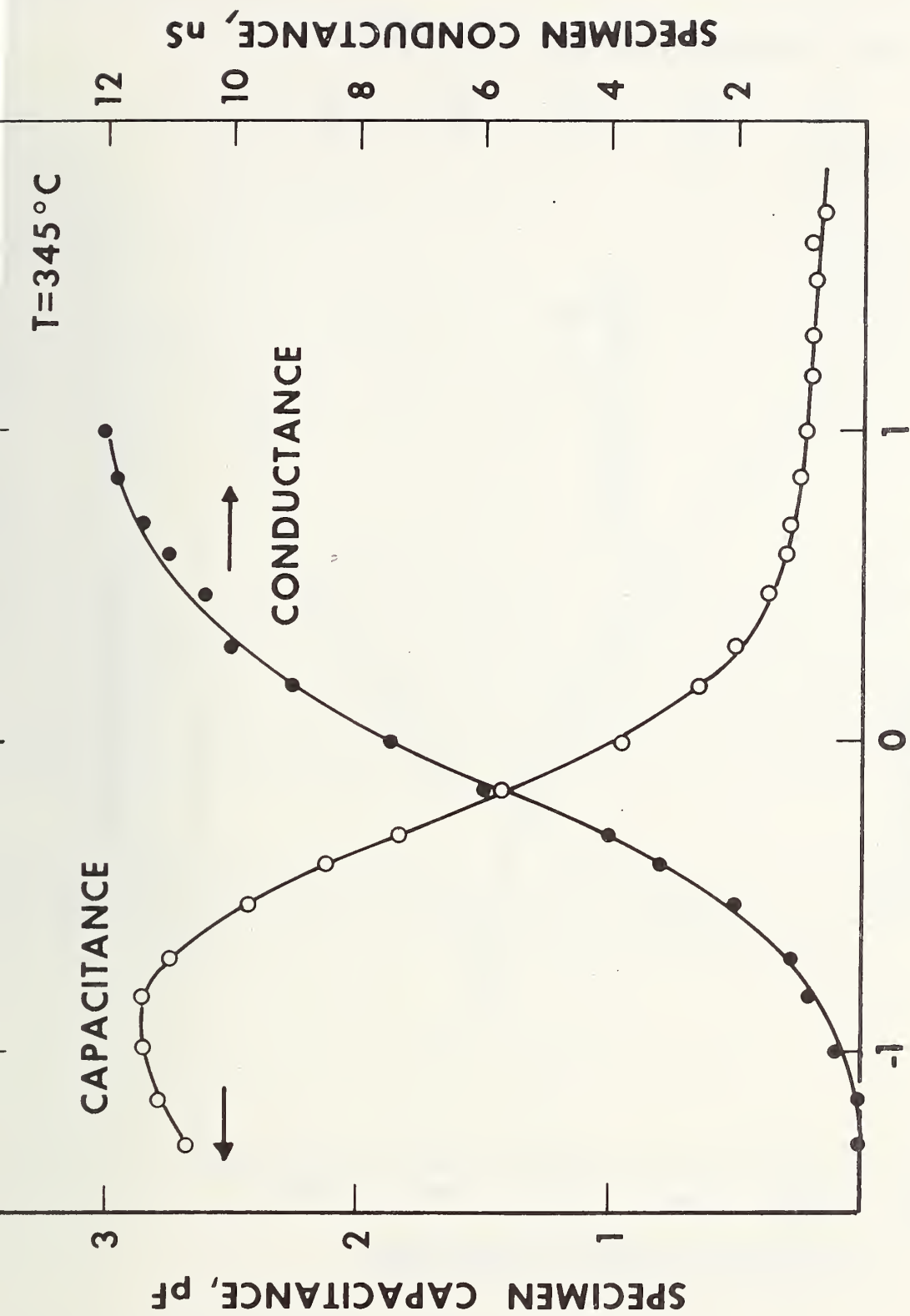
Fig. 7. Frequency dependence of capacitance and conductance of Ca(OH)$_2$ crystal 111-1 at 345° C in all atmospheres. The units of conductance are nanosiemens (see footnote, p. 7).
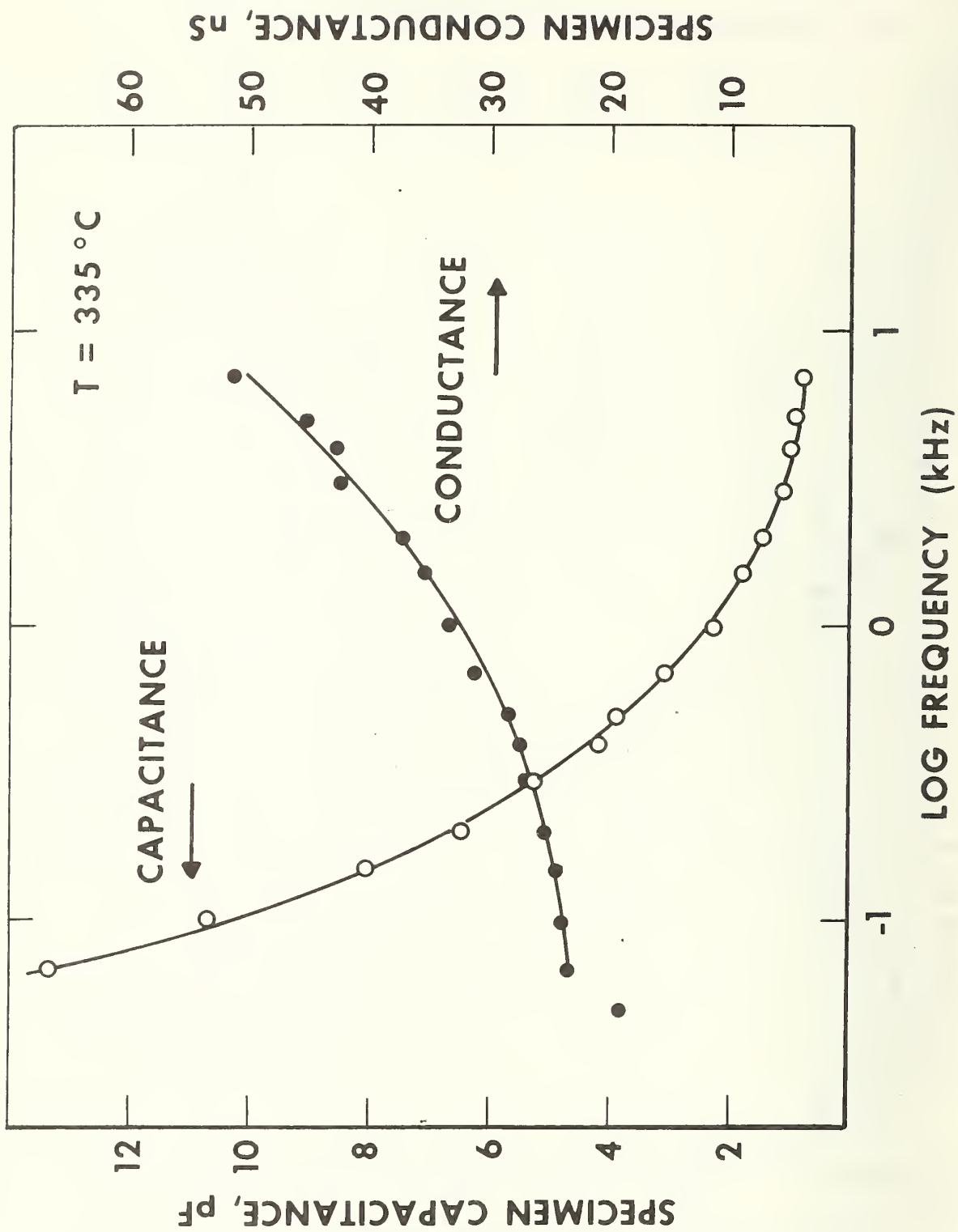
33

Fig. 8. Frequency dependence of capacitance and conductance of $Ca(OH)_2$ crystal 111-2 at 335° C

34

BIBLIOGRAPHIC DATA SHEET	1. Report No. NBSIR 73-404	2.	3. Recipient's Accession No.
4. Title and Subtitle Mass Transport and Physical Properties of Large Crystals of Calcium Apatites: Studies of Ca(OH)$_2$ Crystals for Use in Electrolytic Conversion of Calcium Fluorapatite Crystals to Calcium Hydroxyapatite			5. Report Date Dec 1973 (Date of Issue)
			6.
7. Author(s) A. D. Franklin and K. F. Young			8. Performing Organization Rept. No.
9. Performing Organization Name and Address National Bureau of Standards Department of Commerce Washington, D.C. 20234			10. Project/Task/Work Unit No. 3130457
			11. Contract/Grant No. Y01-DE-30010 Formerly - NIDR10
12. Sponsoring Organization Name and Address National Institute of Dental Research Bethesda, Md. 20014			13. Type of Report & Period Covered Annual, 9/72-8/73
			14.

15. Supplementary Notes

16. Abstracts

In order to convert single crystals of calcium fluorapatite to calcium hydroxyapatite, an electrolytic cell technique will be explored. To utilize such a technique, the cathode compartment must consist of a source of hydroxyl ions and a barrier to the flow of all others. Examination of the literature on metallic hydroxides suggests that a suitable cathode might be composed of an oriented Me(OH)$_2$ crystal, where Me is Mg, Ca, Sr, or Ba, backed up by a Pt electrode in an atmosphere containing H$_2$O and O$_2$. Ca(OH)$_2$ crystals have been grown from aqueous solution, and Pt electrodes evaporated onto them. An apparatus has been built to study their ac admittance as a function of temperature and atmosphere, and measurements begun. A computer program for handling the complex admittance data has been devised and tested.

17. Key Words and Document Analysis. 17a. Descriptors

ac impedance; calcium apatites; calcium hydroxide; crystal growth; electrolysis; interfacial polarization; ionic conduction; mass transport.

17b. Identifiers/Open-Ended Terms

17c. COSATI Field/Group

Availability Statement Release Unlimited	19. Security Class (This Report) UNCLASSIFIED	21. No. of Pages 35
	20. Security Class (This Page) UNCLASSIFIED	22. Price